AIP | Journal of Applied Physics

Effects of a Gaussian size distribution on the absorption spectra of III-V semiconductor quantum dots

Subindu Kumar and Dipankar Biswas

Citation: J. Appl. Phys. **102**, 084305 (2007); doi: 10.1063/1.2798986
View online: http://dx.doi.org/10.1063/1.2798986
View Table of Contents: http://jap.aip.org/resource/1/JAPIAU/v102/i8
Published by the American Institute of Physics.

Effects of a Gaussian size distribution on the absorption spectra of III-V semiconductor quantum dots

Subindu Kumar[a] and Dipankar Biswas
Institute of Radiophysics and Electronics, University of Calcutta, 92 A.P.C. Rd., Kolkata 700009, India

(Received 15 May 2007; accepted 27 August 2007; published online 22 October 2007)

The advancement in the fabrication of low-dimensional semiconductor structures has made it possible to grow zero-dimensional electron-hole systems called quantum dots (QDs). In recent years, there have been extensive studies on III-V semiconductor QDs. In this paper, we have formulated the absorption spectra of realistic QD systems with dot size distribution described by a Gaussian function. The dots were approximated as cubic boxes having finite potentials at the boundaries. The effects of size nonuniformity on the optical absorption spectra of few realistic QD systems were analyzed, and the results have been compared with ideal dots having infinite potentials at the boundaries. © *2007 American Institute of Physics*. [DOI: 10.1063/1.2798986]

I. INTRODUCTION

Quantum dots (QDs), also called zero-dimensional quantum boxes (QBs), of III-V compound semiconductors are being progressively used in the fabrication of optoelectronic devices, such as lasers and detectors, for higher efficiencies and lower threshold currents, taking advantage of the modified density of states in particular. The absorption spectra of QDs are expected to be a series of δ-function-like discrete lines due to the nature of the density of states. There have been constant efforts to utilize QDs and QD systems for infrared detectors.[1–6] The QD system is usually inhomogeneous due to the large variation of the dot size. The spectral response of the detectors utilizing QD systems is subject to change due to the variation of the dot size.[2,6,7] There are reports[8,9] on the effect of a Gaussian distribution of the dot size on the optical absorption spectra. In such investigations, the dots were approximated as cubic or spherical structures having infinite potential barriers at the boundaries. There are reports on electron and hole confinement in QBs.[10–16] Fabricated QDs may be typically circular or lenslike structures rather than square. In some investigations, these dots are approximated as thin quantum boxes.[13,14] Shape effects are minimal for structures with the same cross sectional area.[13] Further, QDs have been previously analyzed with the help of infinite potential barriers;[17–19] realistic semiconductor QDs having finite potential barriers have not been widely discussed or analyzed.

In this paper, we have investigated the optical absorption spectra of realistic semiconductor QD systems with a nonuniform size distribution described by a Gaussian function. We have approximated the QD as a QB with finite potential barriers which may be helpful for a proper analysis of the optical properties of realistic semiconductor QD systems. A comparative study of the ideal and realistic dots was carried out. It is found that the absorption spectra of different realistic III-V compound semiconductor QDs depend strongly on the dot size distribution described by the parameter ξ,[8] the ratio of the standard deviation of the dot size to the average dot size of the system. The results were compared with the ideal dots where we find that the spectra of the realistic dots seem to be redshifted and the linewidth decreases. Further studies on the absorption spectra corresponding to different values of ξ were carried out, and it was found that the resolvability of the absorption peaks depend on ξ. After the statement of the exact nature of the problem and the aim, the paper is to narrate clearly the modification of formulas that had to be done, the computational methodologies, and the results in detail, along with necessary discussions.

II. THEORETICAL MODEL

For a three-dimensional rectangular infinite well, the potential is zero inside the box of side length L_i (where $i=1,2,3$) and infinite outside the box. In such a case, the resulting normalized wave function becomes[14,20]

$$\psi(x) = \sqrt{\frac{8}{L_1 L_2 L_3}} \sin(k_1 x_1)\sin(k_2 x_2)\sin(k_3 x_3), \tag{1}$$

where $k_j = \pi n_j / L_i$ ($n_j = \pm 1, \pm 2, \ldots$) is the wave vector along the x_j direction. For a cubic box of side L, Eq. (1) reduces to[8]

$$\psi(x) = \left(\frac{2}{L}\right)^{3/2} \sin(k_1 x_1)\sin(k_2 x_2)\sin(k_3 x_3). \tag{2}$$

The confinement energies of the electron, $E_e(n^2)$, and that of the hole, $E_h(n^2)$ (in units of $\hbar^2/mL^2$) for a finite well can be approximated as[21]

$$E_e(n^2) = \frac{2P_e^2}{(P_e+1)^2}\left[\left(\frac{n\pi}{2}\right)^2 - \frac{1}{3(P_e+1)^3}\left(\frac{n\pi}{2}\right)^4 - \frac{27P_e - 8}{180(P_e+1)^6}\left(\frac{n\pi}{2}\right)^6\right], \tag{3}$$

$$E_h(n^2) = \frac{2P_h^2}{(P_h+1)^2}\left[\left(\frac{n\pi}{2}\right)^2 - \frac{1}{3(P_h+1)^3}\left(\frac{n\pi}{2}\right)^4 - \frac{27P_h - 8}{180(P_h+1)^6}\left(\frac{n\pi}{2}\right)^6\right], \tag{4}$$

[a]Electronic mail: subindukumar@hotmail.com

$$n^2 = \sum n_j^2, \quad j = 1,2,3, \tag{5}$$

where P_e and P_h are the well strength parameters defined as $P_e = (\sqrt{2m_0 m_e^* V_0/\hbar})L/2$ and $P_h = (\sqrt{2m_0 m_h^* V_0/\hbar})L/2$, where V_0 is the height of the well (conduction/valance band) and L is the well width. m_0, m_e^*, and m_h^* are the rest and effective masses of electrons and holes, respectively. The lowest state corresponds to $n^2=3$. For an infinite deep potential well, $P \to \infty$, and Eqs. (3) and (4) reduces to the well known result,

$$\lim_{P\to\infty} E_e(n^2) = \frac{\pi^2\hbar^2 n^2}{2m_0 m_e^* L^2} \tag{6}$$

and

$$\lim_{P\to\infty} E_h(n^2) = \frac{\pi^2\hbar^2 n^2}{2m_0 m_h^* L^2}. \tag{7}$$

Let us now define the resonance energy of a realistic QD, having finite potential barriers, as the photon energy needed for the creation of an electron-hole pair. This may be represented as

$$\hbar\omega_{\text{real}} = E_g + E_e(n^2) + E_h(n^2), \tag{8}$$

where E_g is the band gap of the semiconductor material. The resonance energy of an ideal dot having infinite potential barriers, $\hbar\omega_{\text{ideal}}$, can be expressed as[8]

$$\hbar\omega_{\text{ideal}} = \lim_{P\to\infty} \hbar\omega_{\text{real}} = E_g + \frac{\pi^2\hbar^2}{2L^2}\left[\frac{1}{m_0 m_e^* + m_0 m_h^*}\right] n^2 = E_g + \frac{\pi^2\hbar^2 n^2}{2\mu L^2}, \tag{9}$$

where $1/\mu = 1/(m_0 m_e^*) + 1/(m_0 m_h^*)$. The optical absorption constant is defined as the ratio of the energy removed from the incident beam per unit time and unit volume to the incident flux.[9] The energy flux is interpreted as the product of the energy density and the speed of flow. Using this definition, the optical absorption coefficient of a realistic cubic dot with length L is calculated as[8]

$$\alpha_{\text{real}} = \frac{A_{\text{real}}}{L^3}\sum_{(n^2)} g(n^2)\,\delta[\hbar\omega_{\text{real}} - \{E_g + E_e(n^2) + E_h(n^2)\}], \tag{10}$$

where $g(n^2)$ is the degeneracy of the energy level determined by $n^2 = \Sigma n_j^2$. Only $\Delta n = 0$ transitions are considered allowed. A_{real} is a constant in terms of the momentum matrix P_n so that[8]

$$A_{\text{real}} = \frac{2\pi e^2 |P_n|^2}{m_0^2 \varepsilon_r^{1/2} \varepsilon_0 c \omega_{\text{real}}}, \tag{11}$$

where e is the fundamental charge, ε_0 is the permittivity of free space, ε_r is the host material, c is the speed of light, and ω_{real} is the photon frequency. Similarly, for an ideal QD system, the optical absorption coefficient can be expressed as[8]

$$\alpha_{\text{ideal}} = \frac{A_{\text{ideal}}}{L^3}\sum_{(n^2)} g(n^2)\,\delta\left[\hbar\omega_{\text{ideal}} - \left(E_g + \frac{\pi^2\hbar^2}{2\mu L^2} n^2\right)\right], \tag{12}$$

where

$$A_{\text{ideal}} = \frac{2\pi e^2 |P_n|^2}{m_0^2 \varepsilon_r^{1/2} \varepsilon_0 c \omega_{\text{ideal}}}. \tag{13}$$

The constant A_{ideal} and the photon frequency ω_{ideal} corresponds to that of an ideal dot having infinite potential barriers. The interband absorption of a QD is characterized by a series of discrete lines at photon energies given by Eqs. (8) and (9). As mentioned by Wu *et al.*,[8] the absorption spectra is the superimposition of the contribution from each individual dot; the overall behavior is modeled by considering a Gaussian distribution of the dot size of side length L, which can be represented as[8]

$$P(L) = \left(\frac{1}{D}\right)\left(\frac{1}{\sqrt{2\pi}}\right)\exp\left[-\frac{(L-L_0)^2}{2D^2}\right], \tag{14}$$

where L_0 is the average dot size of the system and D is the standard deviation. Let ξ be the relative standard deviation of the dot given by

$$\xi = D/L_0, \tag{15}$$

$$\therefore P(L) = \frac{1}{\xi L_0}\frac{1}{\sqrt{2\pi}}\exp\left[-\left(\frac{L}{L_0} - 1\right)^2 \Big/ 2\xi^2\right]. \tag{16}$$

Let us now define two dimensionless parameters: the reduced photon energies x_{real}^2 and x_{ideal}^2 for a realistic and an ideal QD system, respectively, represented as

$$x_{\text{real}}^2 = \frac{\hbar\omega_{\text{real}} - E_g}{[E_e(n^2)_{L=L_0} + E_h(n^2)_{L=L_0}]/n^2} \tag{17}$$

and

$$x_{\text{ideal}}^2 = \frac{\hbar\omega_{\text{ideal}} - E_g}{\pi^2\hbar^2/2\mu L_0^2}. \tag{18}$$

$E_e(n^2)_{L=L_0}$ and $E_h(n^2)_{L=L_0}$ are the values of $E_e(n^2)$ and $E_h(n^2)$ for $L=L_0$. Now, combining Eqs. (12) and (14), the total absorption spectra of an ideal QD system due to the nonuniform dot size distribution is represented as[8]

$$\alpha_{\text{ideal}} = \frac{A_{\text{ideal}}}{D}\frac{1}{\sqrt{2\pi}}\sum_{(n^2)} g(n^2)\int_0^\infty \frac{1}{L^3} e^{-(L-L_0)^2/2D^2} \times \delta\left[\hbar\omega_{\text{ideal}} - \left(E_g + \frac{\pi^2\hbar^2}{2\mu L^2} n^2\right)\right] dL \tag{19}$$

Integrating Eq. (19) and utilizing Eq. (15),

$$\alpha_{\text{ideal}} = \frac{\beta_{\text{ideal}}}{2L_0^3}\sum_{(n^2)} \frac{g(n^2)}{\xi n^2}\exp\left[-\left(\frac{n}{x_{\text{ideal}}} - 1\right)^2 \Big/ 2\xi^2\right], \tag{20}$$

where

$$\beta_{\text{ideal}} = \frac{(1/\sqrt{2\pi})A_{\text{ideal}}}{\pi^2\hbar^2/2\mu L_0^2}. \tag{21}$$

Now, we model the optical absorption spectra of a realistic cubic dot of finite potential barrier at the boundaries as

$$\alpha_{\text{real}} = \frac{\beta_{\text{real}}}{2L_0^3}\sum_{(n^2)} \frac{g(n^2)}{\xi n^2}\exp\left[-\left(\frac{n}{x_{\text{real}}} - 1\right)^2 \Big/ 2\xi^2\right], \tag{22}$$

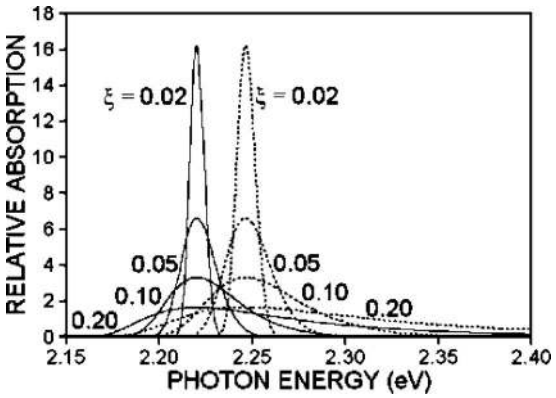

FIG. 1. Absorption spectra of the lowest transition of the $In_{0.7}Ga_{0.3}N/GaN$ QD system corresponding to both real and ideal dots for relative standard deviation ξ=0.02, 0.05, 0.10, and 0.20, as specified. The solid and dotted curves correspond to the realistic and ideal QD systems, respectively. The photon energy for real and ideal dots is defined by Eqs. (8) and (9). The relative absorption of the ideal and realistic dots defined as $\alpha_{\text{real}}/(\beta_{\text{real}}/2L_0^3)$ and $\alpha_{\text{ideal}}/(\beta_{\text{ideal}}/2L_0^3)$ from Eqs. (20) and (22), respectively.

$$\text{where } \beta_{\text{real}} = \frac{(1/\sqrt{2\pi})A_{\text{real}}}{[E_e(n^2)_{L=L_0} + E_h(n^2)_{L=L_0}]/n^2}. \tag{23}$$

In the realm of an ideal cubic QD system, P_e, $P_h \to \infty$ and the photon frequency $\omega=\omega_{\text{ideal}}$ such that

$$\lim_{P_e,P_h\to\infty} \beta_{\text{real}} = \frac{(1/\sqrt{2\pi})A_{\text{ideal}}}{\pi^2\hbar^2/2\mu L_0^2} = \beta_{\text{ideal}}. \tag{24}$$

This agrees with the choice of our denominator of Eq. (23). Equations (20) and (22) represent a set of Gaussian absorption peaks with peak photon energies determined by the average dot size L_0 and represented in Eqs. (8) and (9). The linewidths of the n^2 absorption peak of the ideal and realistic dots, W_{ideal} (Ref. 8) and W_{real}, are given by

$$W_{\text{ideal}} = \frac{4.71\xi}{(1-1.39\xi^2)^2}[n^2\pi^2\hbar^2/2\mu L_0^2], \tag{25}$$

$$W_{\text{real}} = \frac{4.71\xi}{(1-1.39\xi^2)^2}[E_e(n^2)_{L=L_0} + E_h(n^2)_{L=L_0}], \tag{26}$$

and

$$W_{\text{reduction}} = W_{\text{ideal}} - W_{\text{real}}, \tag{27}$$

where $W_{\text{reduction}}$ represents the difference in the linewidths of the n^2 absorption peak of the ideal and realistic dots. It could be inferred from Eqs. (25) and (26) that the linewidth is proportional to the size deviation ξ and approaches zero when $\xi \to 0$. Also, the linewidth is larger for higher transition energy levels.

III. RESULTS AND DISCUSSION

The results of the computations of the absorption spectra of $In_{0.7}Ga_{0.3}N/GaN$ and $In_{0.66}Ga_{0.33}As/GaAs$ QD systems are shown in Figs. 1–3. In each of these figures, the spectra of the realistic and ideal QD system are shown in the same plot. Figure 1 shows the plot of the lowest absorption peak (n^2=3) for $In_{0.7}Ga_{0.3}N/GaN$ QD system with ξ=0.02, 0.04, 0.10, and 0.20. The absorption spectra for the realistic and

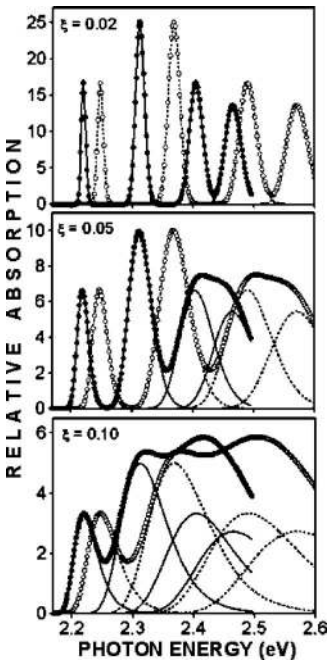

FIG. 2. Absorption spectra of the lowest four transitions of the $In_{0.7}Ga_{0.3}N/GaN$ QD system corresponding to both real and ideal dots. In each of these plots, the solid and dotted lines represent the individual absorption peaks of real and ideal dots, respectively, while the closed and open circle curves correspond to their superposition. The photon energy for real and ideal dots is defined by Eqs. (8) and (9). The relative absorption of the ideal and realistic dots defined as $\alpha_{\text{real}}/(\beta_{\text{real}}/2L_0^3)$ and $\alpha_{\text{ideal}}/(\beta_{\text{ideal}}/2L_0^3)$ from Eqs. (20) and (22), respectively.

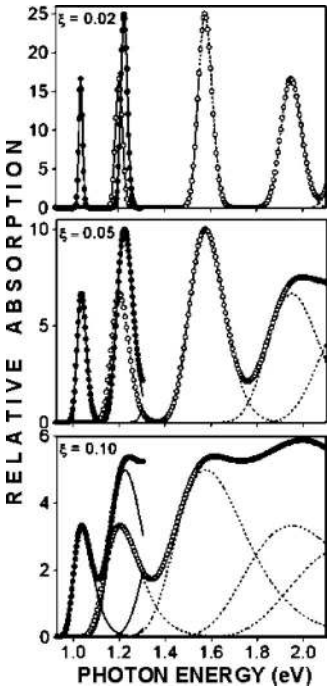

FIG. 3. Absorption spectra of the lowest four transitions of the $In_{0.66}Ga_{0.33}As/GaAs$ QD system corresponding to both real and ideal dots. In each of these plots, the solid and dotted lines represent the individual absorption peaks of real and ideal dots, respectively, while the closed and open circle curves correspond to their superposition. The photon energy for real and ideal dots is defined by Eqs. (8) and (9). The relative absorption of the ideal and realistic dots defined as $\alpha_{\text{real}}/(\beta_{\text{real}}/2L_0^3)$ and $\alpha_{\text{ideal}}/(\beta_{\text{ideal}}/2L_0^3)$ from Eqs. (20) and (22), respectively.

ideal dots are denoted by solid and dotted lines, respectively. The horizontal axis is the photon energy corresponding to real and ideal dots defined by Eqs. (8) and (9), respectively. The vertical axis is the relative absorption of the ideal and realistic dots defined as $\alpha_{\text{real}}/(\beta_{\text{real}}/2L_0^3)$ and $\alpha_{\text{ideal}}/(\beta_{\text{ideal}}/2L_0^3)$ according to Eqs. (20) and (22).

For the $In_{0.7}Ga_{0.3}N/GaN$ QD system, the energy band gap of $In_xGa_{1-x}N$, E_g, was calculated from the equation[22]

$$E_g(x) = (1-x)E_{g,\text{GaN}} + xE_{g,\text{InN}} - bx(1-x), \tag{28}$$

where x is the mole fraction of indium, $E_{g,\text{GaN}}$ and $E_{g,\text{InN}}$ are the energy band gaps of GaN and InN, respectively, and b is the bowing parameter. In our calculation $E_{g,\text{GaN}}$, $E_{g,\text{InN}}$, x, and b were assumed to be 3.4 eV, 2 eV, 0.7, and 1.4, respectively. Considering $x=0.7$, the band gap $E_{g,\text{InGaN}}$ comes out to be 2.126 eV. For finite potential barriers, considering the band offset ratio to be 55: 45,[23] the conduction and valance band heights were found to be 0.701 and 0.573 eV. The average dot size was considered to be 7.25 nm. The effective masses are assumed to be $0.2m_0$ for electrons[22] and $1.56m_0$ for heavy holes.[24] The computed absorption spectra of the $In_{0.7}Ga_{0.3}N/GaN$ QD system is shown in Fig. 2.

There are reports on the growth of $In_{0.66}Ga_{0.33}As/GaAs$ QDs.[25] The computed absorption spectra of such QD ensemble is shown in Fig. 3. The band gap, $E_{g,\text{InGaAs}}$, of $In_xGa_{1-x}As$ is determined from the empirical relation[26]

$$E_{g,\text{InGaAs}} = 1.516 - 1.214x + 0.264x^2, \tag{29}$$

where x is the concentration of indium. The effective masses[27] were taken to be $0.041m_0$ for electrons and $0.417m_0$ for holes, which were obtained through a linear extrapolation between the effective masses of InAs and GaAs. $E_{g,\text{InGaAs}}$ and the band offset ratio were considered to be 0.830 eV and 60:40, respectively. For realistic dots, the well heights of the conduction and valance bands were found to be 0.412 and 0.274 eV, respectively. The average dot size was considered to be 9 nm.

The ranges of photon energies in Figs. 2 and 3 were so chosen so as to accommodate the lowest four transitions. The solid line and the filled circles represent the individual absorption peaks and their superposition of the realistic dots, respectively, while for ideal dots it is represented by dotted lines and open circles. In both the cases, with $\xi=0.02$, all the peaks could be resolved. As ξ increases, the resolvability decreases. It should be noted at this juncture that for the $In_{0.66}Ga_{0.33}As/GaAs$ QD system the curves could not be extended beyond a certain energy (1.302 eV) since the confinement energies exceeded the height of the well and only the lowest two transitions could be observed, as shown in Fig. 3. This problem is not encountered in the case of the $In_{0.7}Ga_{0.3}N/GaN$ QD system, and the lowest four transitions could be accommodated, as depicted in Fig. 2.

It is observed that for realistic dots, there is a redshift of the absorption peaks and there is a decrease in the linewidth as compared to the ideal QD system for the same size deviation. The photon energies corresponding to the Gaussian absorption peaks depend on the band gap of the semiconductor material and the confinement energies of the conduction and the valance bands. For realistic dots having a finite potential barrier, the confinement energies are less as compared to ideal dots having infinite potential barriers. As a result, the absorption peaks suffer from a redshift. The variation of the energy of the subbands with change in the size of the dots is much more pronounced in the case of infinite wells as compared to finite wells. Hence, larger deviation in the absorption energies for a particular ξ is expected in the case of infinite wells, and hence the absorption spectra become broader. Moreover, in a narrow finite well less number of levels will be available for transitions, which will make the spectrum narrow. The computed values of the difference in the linewidth of ideal and realistic $In_{0.7}Ga_{0.3}N/GaN$ and $In_{0.66}Ga_{0.33}As/GaAs$ QD systems for the lowest three transitions are depicted in Table I. For the $In_{0.66}Ga_{0.33}As/GaAs$ QD system, the data corresponding to the lowest two transitions could only be computed since the absorption spectra corresponding to the higher order transitions were found to be absent, as shown in Fig. 3. It is also observed that the redshift is more pronounced for a smaller average dot size, as shown in Fig. 4. In Fig. 4, the redshift corresponds to the energy difference of the absorption peak of the ideal and realistic dots. Computations were carried out for $\xi=0.05$, where the lowest two transitions could be well resolved. In the case of the $In_{0.7}Ga_{0.3}N/GaN$ QD system, due to the relatively small well height, the redshift corresponding to the second transition level could be obtained only after a certain average dot size. Figure 5 shows the dependence of the line-

TABLE I. Difference in the linewidth, $W_{\text{reduction}}$, of the n^2 absorption peak of ideal and realistic $In_{0.7}Ga_{0.3}N/GaN$ and $In_{0.66}Ga_{0.33}As/GaAs$ QD systems computed from Eq. (27) for $\xi=0.02$ and $\xi=0.05$.

	Linewidth reduction			
	$In_{0.7}Ga_{0.3}N/GaN$		$In_{0.66}Ga_{0.33}As/GaAs$	
Transition	$\xi=0.02$ $W_{\text{reduction}}$ (eV)	$\xi=0.05$ $W_{\text{reduction}}$ (eV)	$\xi=0.02$ $W_{\text{reduction}}$ (eV)	$\xi=0.05$ $W_{\text{reduction}}$ (eV)
First ($n^2=3$)	0.002	0.007	0.015	0.039
Second ($n^2=6$)	0.006	0.013	0.033	0.083
Third ($n^2=9$)	0.008	0.030	...	...

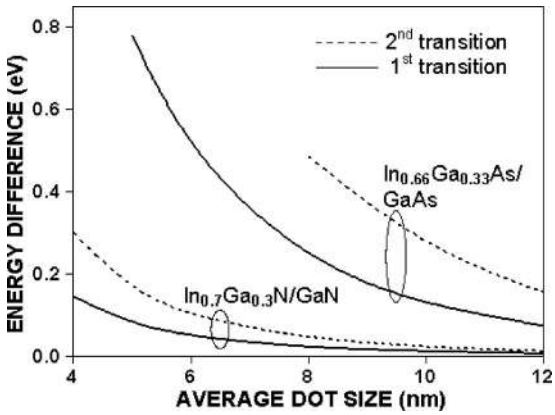

FIG. 4. Variation of the energy difference of the absorption peak of the ideal and realistic dots with average dot size. Results of computations are presented for both $In_{0.7}Ga_{0.3}N/GaN$ and $In_{0.66}Ga_{0.33}As/GaAs$ QD systems for the lowest two transitions.

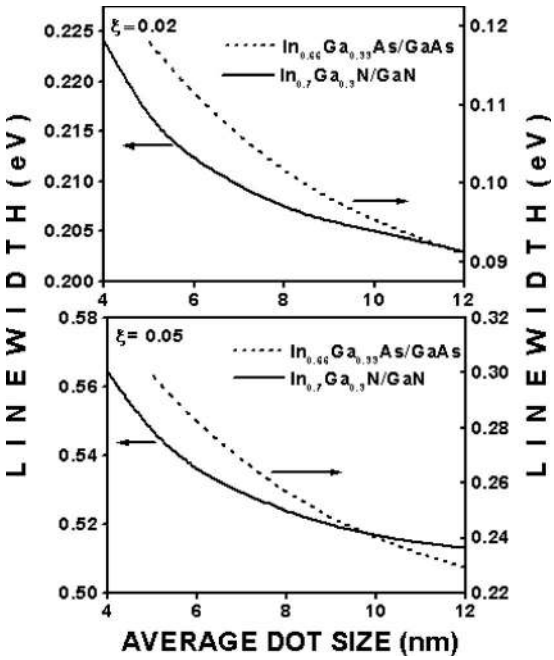

FIG. 5. Variation of the linewidth of realistic QD systems on the average dot size for $\xi=0.02$ and 0.05. The linewidth is defined by Eq. (26), and the results of the computations are presented for both $In_{0.7}Ga_{0.3}N/GaN$ and $In_{0.66}Ga_{0.33}As/GaAs$ realistic QD systems for the lowest transition.

width of realistic dots on the average dot size for $\xi=0.02$ and 0.05. The linewidth is defined by Eq. (26), and the results of computations are presented for both $In_{0.7}Ga_{0.3}N/GaN$ and $In_{0.66}Ga_{0.33}As/GaAs$ realistic QD systems for the lowest transition. It is observed that the linewidth falls rapidly in the case of smaller average dot size and seems to saturate as the average dot size increases.

IV. SUMMARY

To summarize, a model has been formulated to investigate the interband optical absorption of realistic QD systems having finite potentials at the boundaries. Considering the Gaussian distribution of the dot size, the absorption spectra of $In_{0.7}Ga_{0.3}N/GaN$ and $In_{0.66}Ga_{0.33}As/GaAs$ QD systems have been calculated, where it is observed that for realistic dots there is a redshift of the absorption peak and the linewidth decreases as compared to that of the ideal QD system for the same size deviation.

[1]H. C. Liu, M. Gao, J. McCaffrey, Z. R. Wasilewski, and S. Farad, Appl. Phys. Lett. **78**, 79 (2001).
[2]Y. H. Kang, J. Park, U. H. Lee, and S. Hong, Appl. Phys. Lett. **82**, 1099 (2003).
[3]J. Phillips, P. Bhattacharya, S. W. Kennerly, D. W. Beckman, and M. Dutta, IEEE J. Quantum Electron. **35**, 936 (1999).
[4]J. Phillips, J. Appl. Phys. **91**, 4590 (2002).
[5]S. Krishna, O.-H. Kwon, and M. M. Hayat, IEEE J. Quantum Electron. **41**, 1468 (2005).
[6]V. Apalkov, J. Appl. Phys. **100**, 076101 (2006).
[7]B. Pattada, J. Chen, Q. Zhou, M. O. Manasreh, M. L. Hussein, W. Ma, and G. J. Salamo, Appl. Phys. Lett. **82**, 2509 (2003).
[8]W.-Y. Wu, J. N. Schulman, T. Y. Hsu, and U. Efron, Appl. Phys. Lett. **51**, 710 (1987).
[9]D. L. Ferreira and J. L. A. Alves, Nanotechnology **15**, 975 (2004).
[10]M. Asada, Y. Miyamoto, and Y. Suematsu, IEEE J. Quantum Electron. **QE-22**, 1915 (1986).
[11]J. Cibert, P. M. Petroff, G. J. Dolan, S. J. Pearton, A. C. Gossard, and J. H. English, Appl. Phys. Lett. **49**, 1275 (1986).
[12]M. Michel, A. Forchel, and F. Faller, Appl. Phys. Lett. **70**, 393 (1997).
[13]G. W. Bryant, Phys. Rev. B **37**, 8763 (1988).
[14]H. Gotoh, H. Ando, and H. Kanbe, Appl. Phys. Lett. **68**, 2132 (1996).
[15]T. Aizawa, K. Shimomura, S. Arai, and Y. Suematsu, IEEE Trans. Electron Devices **38**, 2709 (1991).
[16]G. Tsvid, M. D'Souza, D. Botez, B. Hawkins, A. Khandekar, T. Kuech, and P. Zory, J. Vac. Sci. Technol. B **22**, 3214 (2004).
[17]K. J. Vahala, IEEE J. Quantum Electron. **24**, 523 (1988).
[18]Y. C. Chua, E. A. Decuir, Jr., B. S. Passmore, K. H. Sarif, M. O. Manasreh, Z. M. Wang, and G. J. Salamo, Appl. Phys. Lett. **85**, 1003 (2004).
[19]For example, see D. Bimberg, M. Grundmann, and N. N. Ledentsor, *Quantum Dot Heterostructures* (Wiley, Chichester, 1999).
[20]For example, see D. J. Griffiths, *Introduction to Quantum Mechanics*, 2nd ed. (Prentice-Hall, Englewood Cliffs, NJ, 2004).
[21]D. L. Aronstein and C. R. Stroud, Jr., Am. J. Phys. **68**, 943 (2000).
[22]S. Nakamura, T. Mukai, M. i Senoh, Shin-ichi Nagahama, and N. Iwasa, J. Appl. Phys. **74**, 3911 (1993).
[23]D. Biswas, S. Kumar, and T. Das, Thin Solid Films **515**, 4488 (2007).
[24]C.-C. Chen, H.-W. Chuang, G.-C. Chi, C.-C. Chuo, and J.-I. Chyi, Appl. Phys. Lett. **77**, 3758 (2000).
[25]G. E. Cirlin, V. N. Petrov, V. G. Dubrovskii, A. O. Golubox, S. Y. Tipissev, G. M. Guryanov, M. V. Maximov, N. N. Ledentsov, and D. Bimberg, Czech. J. Phys. **47**, 379 (1997).
[26]W. P. Gillin, D. J. Dunstan, K. P. Homewood, L. K. Howard, and B. J. Sealy, J. Appl. Phys. **73**, 3782 (1993).
[27]For example, see *Data in Science and Technology, Semiconductors Group IV Elements and III-V Compounds*, edited by O. Madelung (Springer-Verlag, Berlin, 1991).